Blasco-Brusola, A.; Vayá Pérez, I.; Miranda Alonso, MÁ. (2020). Regioselectivity in the adiabatic photocleavage of DNA-based oxetanes. Organic & Biomolecular Chemistry. 18(44):9117-9123. https://doi.org/10.1039/D0OB01974G

ARTICLE

Regioselectivity in the adiabatic photocleavage of DNA-based oxetanes

Received 00th January 20xx,
Accepted 00th January 20xx

DOI: 10.1039/x0xx00000x

Alejandro Blasco-Brusola, Ignacio Vayá* and Miguel A. Miranda*

Direct absorption of UVB light by DNA may induce formation of cyclobutane pyrimidine dimers and pyrimidine-pyrimidone (6-4) photoproducts. The latter arise from the rearrangement of unstable oxetane intermediates, which have also been proposed to be the electron acceptor species in the photoenzymatic repair of this type of DNA damage. In the present work, direct photolysis of oxetanes composed of substituted uracil (Ura) or thymine (Thy) derivatives and benzophenone (BP) have been investigated by means of transient absorption spectroscopy from the femtosecond to the microsecond time-scales. The results showed that photoinduced oxetane cleavage takes place through an adiabatic process leading to the triplet excited BP and the ground state nucleobase. This process was markedly affected by the oxetane regiochemistry (head-to-head, HH, *vs*. head-to-tail, HT) and by the nucleobase substitution; it was nearly quantitative for all investigated HH-oxetanes while it became strongly influenced by the substitution at positions 1 and 5 for the HT-isomers. The obtained results clearly confirm the generality of the adiabatic photoinduced cleavage of BP/Ura or Thy oxetanes, as well as its dependence on the regiochemistry, supporting the involvement of triplet exciplexes. As a matter of fact, when formation of this species was favored by keeping together the Thy and BP units after splitting by means of a linear linker, a transient absorption at ~400 nm, ascribed to the exciplex, was detected.

Introduction

The origin of human diseases such as skin cancer can be associated in many cases to photoinduced DNA damage.[1-3] Thus, when DNA absorbs UV light, a cascade of reactions may lead to the formation of cyclobutane pyrimidine dimers (CPDs) and to a lesser extent pyrimidine-pyrimidone (6-4) photoproducts ((6-4)PPs), which may result in the appearance of mutations and cell death.[4-7] The CPD photolesions can also arise from photosensitization, where an endogenous or exogenous photosensitizer (PS) can absorb UVA light to generate long-lived reactive species such as excited triplet states that will be the initiators of the damaging reactions.[8, 9] Nature has developed efficient mechanisms to repair these lesions. In this context, the nucleotide excision repair operates in humans, while in other organisms such as bacteria or plants the involvement of a photolyase reverses the damage through a photoinduced electron transfer process.[10-13]

Benzophenone (BP) is a well-known photosensitizing moiety that is present in a variety of drugs.[14] It can induce damage to DNA, and its main target is the thymine (Thy) nucleobase.[15-17] In this regard, excitation of BP with UVA light generates its triplet excited state (^{3}BP*), which can then induce formation of CPDs through a formal [2+2] cycloaddition between two adjacent thymine units, or alternatively it may lead to oxetane derivatives through a triplet exciplex ^{3}[BP···Thy]*.[18-20]

The photoreactivity of monomeric pyrimidine bases such as thymine or uracil (Ura) interacting with BP is highly influenced by the substituents at position C5 of the nucleobase, mainly due to steric hindrance. In this context, CPDs formation in solutions containing BP and Ura derivatives is completely blocked by the presence of a bulky group at the C5 position of the nucleobase.[21] In connection with oxetanes, the Paternò-Büchi photoreaction between Thy and BP derivatives has been reported in the course of model studies related to the photoenzymatic repair of DNA (6-4)PPs.[22-27] Interestingly, direct photolysis of some of these oxetanes results in a rare adiabatic cleavage to form ^{3}BP* and Thy in its ground state.[23, 26] This process has recently been investigated in detail for two head-to-head (HH) and head-to-tail (HT) oxetane regioisomers obtained from 1,3-dimethylthymine (DMT) and BP (see Scheme 1).[18] Irradiation of any of the two isomers induces instantaneous formation of its first excited singlet state, which rapidly evolves to a singlet biradical through C-C bond scission. For the HH- isomer, step (III) to reach the excited triplet exciplex ^{3}[BP···DMT]* has been found to be much more efficient than for the HT-isomer, which may follow step (IV) to generate a triplet biradical that evolves to regenerate either the starting oxetane or the separated Thy and BP chromophores in the ground state. Alternatively, the triplet exciplexes are also formed from the HT oxetane, albeit to a lesser extent; these species finally dissociate to give ^{3}BP* and DMT in the ground state. Consequently, the adiabatic cycloreversion of the two investigated oxetanes seems to be markedly influenced by the HH- *vs.* the HT-regiochemistry.

Departamento de Química/Instituto de Tecnología Química UPV-CSIC, Universitat Politècnica de València, Camino de Vera s/n, 46022 València (Spain).

Electronic Supplementary Information (ESI) available: Synthesis and characterization of the uracil and thymine derivatives and the corresponding intermediates by means of ^{1}H and ^{13}C NMR and HRMS. Synthetic schemes, femtosecond transient absorption and laser flash photolysis spectra and kinetic traces.

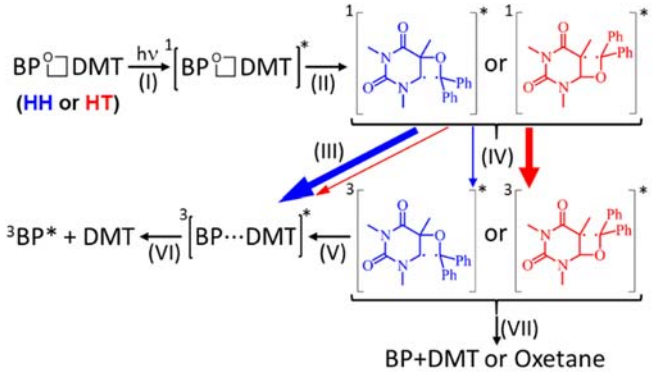

Scheme 1 Schematic representation of the photoinduced cycloreversion process of the HH and HT oxetanes composed of BP and DMT.[18] For clarification, the HH regioisomer follows the blue arrows, while the HT oxetane follows the red ones.

With this background, the aim of the present work is to establish the generality and scope of the adiabatic cycloreversion process and to gain further insight into its mechanistic features, using a variety of oxetanes with different regiochemistries and substitution patterns at positions 1 and 5 of the nucleobase. With this goal, different oxetanes have been obtained by the intermolecular photoreaction between BP and Ura or Thy derivatives. In addition, oxetanes arising from the analogous intramolecular process between Thy and BP units covalently connected by spacers of different nature have also been studied in order to evaluate the possible influence of the linker on the photolytic splitting. Thus, the photobehavior of a variety of HH- and HT-oxetanes (see Fig. 1) has been investigated by means of nanosecond laser flash photolysis (LFP) and, in some cases, femtosecond transient absorption spectroscopy. As a matter of fact, the obtained results confirm the generality of the adiabatic photocleavage in Thy/BP oxetanes, as well as its dependence on the HH- *vs*. HT regiochemistry. Moreover, they indicate that the ring opening process is highly influenced by the nature of the substituents at positions 1 and 5 of the nucleobase.

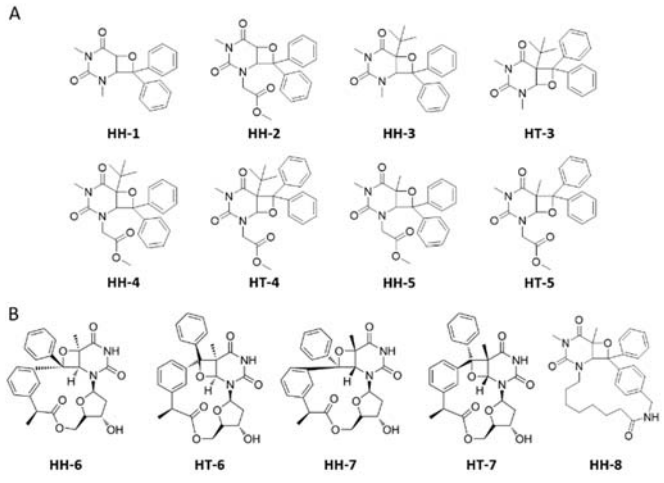

Fig. 1 Chemical structure of the investigated systems. A) Oxetanes arising from the intermolecular photoreaction between BP and Ura (from HH-1 to HT-4) or Thy (HH-5 and HT-5) derivatives. B) Oxetanes arising from the intramolecular photoreaction between BP and Thy units covalently linked by spacers of different nature.

Results and discussion

The photobehavior of oxetanes resulting from the intermolecular photoreaction between BP and Ura or Thy derivatives (see Fig. 1A) was studied first. In general, for all investigated systems, direct steady-state photolysis with UVC light gave rise to the starting materials BP and the Ura or Thy derivatives as the only photoproducts. The synthesis of HH-1 has been described earlier;[28] however, we have slightly modified the synthetic procedure to get the different HH- and HT-regioisomers (see Scheme 2). Briefly, solutions containing BP (0.2 M) and the nucleobase derivative (0.1 M) in acetonitrile were placed into Pyrex tubes and irradiated *ca*. 6h under nitrogen in a Luzchem photoreactor emitting at λ_{max} = 350 nm (12 × 8 W lamps). The crudes were purified by column chromatography to get the final HH- and/or HT-oxetanes as white solids. The synthesis of the precursor nucleobase derivatives is explained in detail in the ESI.

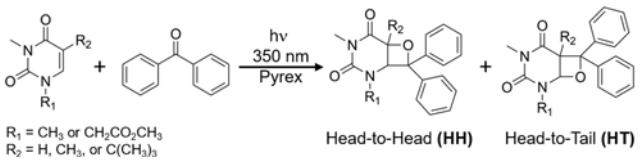

Scheme 2 Schematic representation of the photoinduced cycloreversion process of oxetanes composed of BP and DMT.

Due to the chemical instability of the uracil-derived HT-1 and HT-2, which could not be isolated in pure form, only the photophysical properties of their HH-regioisomers were investigated. Thus, nanosecond laser flash photolysis (LFP) measurements were performed upon excitation at 266 nm in deaerated acetonitrile, using BP as a reference. Under these conditions, photolysis of either HH-1 or HH-2 resulted in the instantaneous formation of a transient absorption peaking at 530 nm, where ^{3}BP* displays its maximum.[29] This result agrees well with the previous observations for the HH BP-DMT oxetane.[18] Thus, after the laser pulse, a nearly quantitative adiabatic population of ^{3}BP* was achieved for both oxetanes (see Fig. 2). The decay traces were properly fitted by a one-order exponential law with lifetimes of about 5 μs for BP and HH-1 and shorter for HH-2 (*ca*. 2 μs). The difference in the triplet lifetimes could be associated with a faster BP triplet quenching by HH-2 than by HH-1.

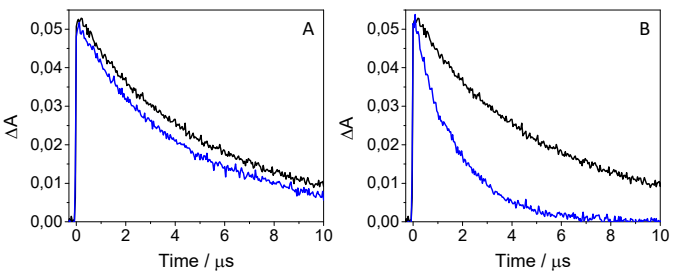

Fig. 2 LFP decay traces at 530 nm for A) HH-1 (blue) and BP (black), and B) HH-2 (blue) and BP (black) after excitation at 266 nm in deaerated acetonitrile.

Since the influence of the regiochemistry on the photobehavior of the HT-uracil derivatives could not be evaluated due to their chemical instability, two additional and more stable substituted uracil oxetanes, namely HH-3 and HT-3, were synthesized with a bulky *tert*-butyl group at position 5. In this context, LFP measurements evidenced clear differences between the two regioisomers (see Fig. 3). Analysis of the kinetic traces at 530 nm showed again an almost quantitative end-of-pulse adiabatic population of ^{3}BP* for HH-3, while this process was much less efficient (*ca*. 35%) for HT-3. Therefore, a strong regioselectivity was observed in the photoinduced ring-opening reaction, which is in line with the results recently reported for the HH and HT BP-DMT oxetanes;[18] noteworthy, in the case of 3 the difference in the degree of adiabaticity found between the HH- and the HT-regioisomers was markedly enhanced. Thus, the presence of a *tert*-butyl substituent at position 5 had little if any effect on the photoreactivity of the HH derivative, but it clearly affected the photobehavior of the HT-isomer.

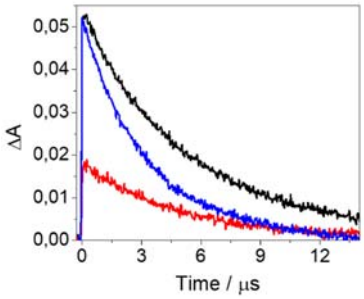

Fig. 3 LFP decay traces at 530 nm for BP (black), HH-3 (blue) and HT-3 (red) after excitation at 266 nm in deaerated acetonitrile.

In order to complete the picture on the influence of the substituents at positions 1 or 5 on the adiabatic cycloreversion of nucleobase-derived oxetanes, two additional uracil-derived compounds were synthesized, namely HH-4 and HT-4 (with a bulky *tert*-butyl substituent at position 5 and a methyl acetate group at position 1) as well as the corresponding Thy analogues HH-5 and HT-5. As stated above for the related compounds HH-3 and HT-3, the ns LFP decay traces at 530 nm for HH-4 and HT-4 (Fig. S11A in ESI) evidenced a remarkable regioselectivity (end-of-pulse ^{3}BP* ratio *ca.* 4:1) in the adiabatic cycloreversion of the investigated oxetanes. Thus, replacement of the methyl group with a methyl acetate substituent at position 1 for the *tert*-butyl derivatives mainly affected the adiabaticity of the HT-isomer, which decreased from 35% in HT-3 to 20% in HT-4. This could be associated with a possible stabilization of the triplet biradical (see Scheme 1) by the influence of the methyl acetate moiety, which could hinder formation of the triplet exciplex (step III) thus favoring step VII to generate the starting oxetane HT-4 or the separated BP and Thy chromophores in the ground state. For the thymine derivatives HH-5 and HT-5 (Fig. S11B in ESI), a regiodifferentiation was again observed in the adiabatic ring-opening (end-of-pulse ^{3}BP* ratio *ca.* 7:3), which was comparable to the results recently reported for BP-DMT oxetanes.[18]

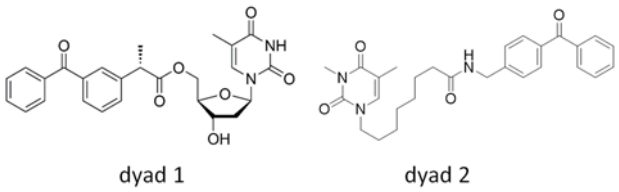

Fig. 4 Chemical structures of dyad 1 and dyad 2.

In view of the photoreactivity observed for the nucleobase-derived oxetanes as a function of the substitution at positions 1 and 5, the photobehavior of polycyclic oxetanes (see Figure 1B) whose splitting could lead to BP and Thy chromophores covalently linked through a spacer of different nature was also investigated. Their synthesis was achieved following the reported procedures,[26, 30] by means of the Paternò-Büchi photoreaction between the BP and Thy units of the precursor dyads 1 and 2 (see Fig. 4). Thus, photolysis of the dyad 1 containing the BP and Thy chromophores linked through a sugar moiety resulted in the formation of HH-6, HT-6, HH-7 and HT-7,[26] whereas HH-8 was obtained from irradiation of dyad 2, where BP and Thy are connected through a linear chain of ten linking atoms.[30] Steady state photolysis of oxetanes HH-6, HT-6, HH-7 and HT-7 gave rise in all cases to dyad 1 as the only photoproduct, whereas, under the same conditions, oxetane HH-8 led cleanly to dyad 2.

Since the lifetime of ^{3}BP* in dyad 1 was very short (~20 ns),[26] reliable transient absorption experiments could only be performed in the femtosecond time-scale. Under the employed experimental conditions, the degree of photodegradation was kept below 5%. As it is shown in Fig. 5, excitation of the different regio- and stereoisomeric oxetanes HH-6, HT-6, HH-7 and HT-7 at 280 nm in acetonitrile led to the formation of the typical triplet-triplet absorption band of BP (see Fig. S12 in ESI);[31, 32] with maximum at *ca.* 530 nm with a time constant of about 9.5 ps. Accordingly, the photoinduced cycloreversion for the intramolecular oxetanes HH-6, HT-6, HH-7 and HT-7 also operates as an adiabatic process.

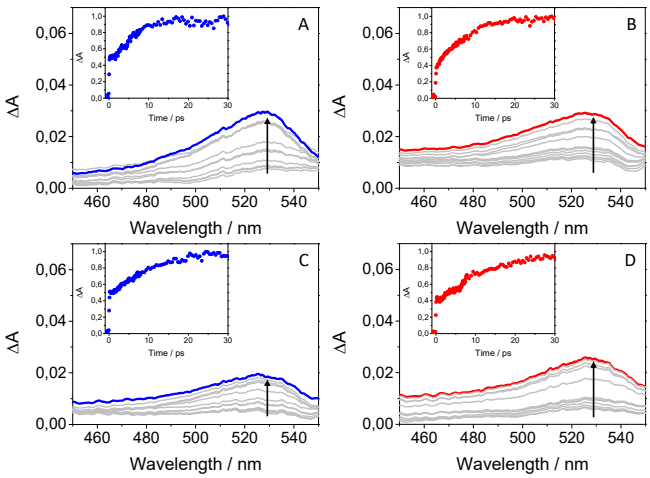

Fig. 5 Femtosecond transient absorption spectra from 0.5 to 40 ps for A) HH-6, B) HT-6, C) HH-7 and D) HT-7. The insets show the kinetic traces at 530 nm. All measurements were performed at λ_{exc} = 280 nm in acetonitrile.

Finally, the photophysical properties of HH-8 were investigated and compared to those of dyad 2.[30] Kinetic analysis of the transient peaking at 530 nm in the ns-μs time-scale upon LFP at 266 nm revealed that the decay traces in both systems could be fitted by a

first order exponential law, with lifetimes of *ca*. 55 ns. More interestingly, HH-8 evidenced once more a complete adiabatic photoreversion process (see Fig. S13 in ESI). However, the spectra and the decay traces were noisy, due to the short triplet lifetime compared to the duration of the pulse. Hence, oxetane HH-8 was also submitted to femtosecond transient absorption measurements (λ_{exc} = 280 nm), which fully confirmed formation of the triplet excited state of the BP-derived chromophore with maximum at *ca*. 530 nm[30] (see Fig. 6A and B). As previously observed for the BP-DMT regioisomers,[18] an absorption at about 400 nm with a flat profile, which is absent for the BP-derived chromophore, was formed in *ca*. 3.5 ps (see Fig. 6C and D); this can be associated with the formation of an intermediate excited triplet exciplex between the BP and Thy chromophores (see Scheme 1).

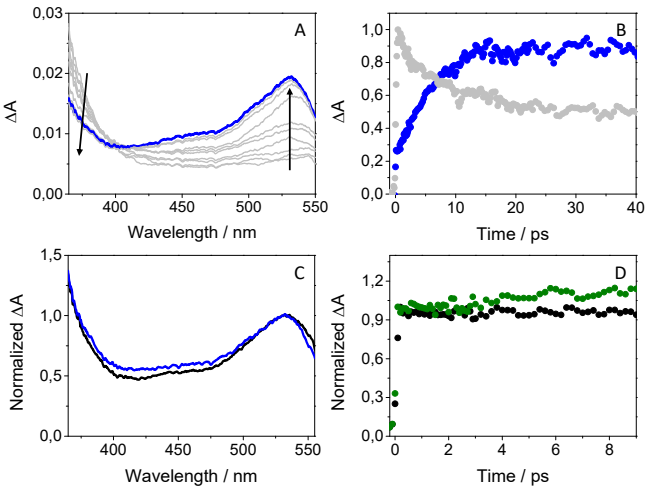

Fig. 6 Femtosecond transient absorption measurements after excitation at 280 nm in acetonitrile: A) spectra from 0.5 to 40 ps and B) kinetic traces at 340 nm (gray) and 530 nm (blue) for HH-8; C) spectra recorded at 10 ps for the BP-derived chromophore (black) and HH-8 (blue); D) kinetic traces at 400 nm for the BP-derived chromophore (black) and HH-8 (green).

In summary, photolysis of the investigated oxetanes resulted in an adiabatic population of ^{3}BP* after ring opening. In this context, a strong regioselectivity was detected for the oxetanes **1-5**, being the degree of adiabaticity much higher for the HH than for the HT isomers (see Table 1). In addition, the process was significantly affected by the substitution at position N1 and C5 of the nucleobase for the HT derivatives, whereas a less marked effect was noticed for the HH isomers.

Table 1 Relationship between the degree of adiabaticity and the substitution at positions N1 and C5 of the nucleobase for the photoreversion of the indicated oxetanes

	Substituent at N1	Substituent at C5	Adiabaticity (%)
HH-1	CH_3	H	100
HH-2	$CH_2CO_2CH_3$	H	100
HH-3	CH_3	*tert*-Bu	100
HT-3	CH_3	*tert*-Bu	35
HH-4	$CH_2CO_2CH_3$	*tert*-Bu	100
HT-4	$CH_2CO_2CH_3$	*tert*-Bu	20
HH-5	$CH_2CO_2CH_3$	CH_3	75
HT-5	$CH_2CO_2CH_3$	CH_3	38

Likewise, the photoinduced cleavage of the polycyclic oxetanes was found to occur as an adiabatic process. Interestingly, for the tricyclic oxetane HH-8, a transient absorption at ~400 nm is detected, which is ascribed to formation of the purported triplet exciplex between the linked benzophenone and thymine chromophores.

Conclusions

The UV-induced photocleavage of a variety of oxetanes arising from the inter- or intramolecular Paternò-Büchi photoreaction between BP and Ura or Thy chromophores has been investigated by means of transient absorption spectroscopy from the femtosecond to the microsecond time-scales. In all cases, an adiabatic process is observed, which leads to the BP unit in its triplet excited state. The degree of adiabaticity depends on the oxetane regiochemistry and on the substitution pattern at positions 1 and 5 of the nucleobase. In general, a nearly quantitative adiabatic cycloreversion is observed for the HH-regioisomers; by contrast, for the HT-oxetanes the process is not fully adiabatic and becomes strongly influenced by the nature of the substituents at positions 1 and 5. The highest regiodifferentiation (4:1 ratio) is detected between HH-4 and HT-4. These results are consistent with the intermediacy of a triplet exciplex, whose formation is more favorable in the HH-regioisomers. In summary, the adiabatic cycloreversion of oxetanes derived from aromatic ketones and pyrimidine bases appears to be a rather general process, which occurs in all the investigated compounds. Regioselectivity (HH *vs.* HT) and substitution-dependence are interesting features of this process.

Experimental section

Chemicals and reagents. 1,3-dimethyluracil, benzophenone (BP), dimethyl sulphate, lithium diisopropylamide (LDA), ethyl formate 97%, thiourea, chloroacetic acid, thymine-1-acetic acid, ethyl bromoacetate, ethyl 4-bromobutyrate, were purchased from Sigma-Aldrich. Ethyl-8-bromooctanoate was purchased from Fluorochem. Methyl 3,3-dimethylbutanoate was purchased from Alfa-aesar. Sodium hydroxide (NaOH), potassium hydroxide (KOH), magnesium sulphate ($MgSO_4$), hydrochloric acid 37% (HCl) and acetonitrile spectroscopic grade were purchased from Scharlab.

Spectroscopic Techniques. The ^{1}H NMR and ^{13}C NMR spectra were recorded at 400 and 100 MHz, respectively, using a Bruker AVANCE III instrument; chemical shifts are reported in ppm.

High-resolution mass spectrometry (HRMS) was performed in an Ultra Performance Liquid Chromatography (UPLC) ACQUITY system (Waters Corp.) with a conditioned autosampler at 4 °C. The separation was accomplished on an ACQUITY UPLC BEH C18 column (50 mm × 2.1 mm i.d., 1.7 µm), which was maintained at 40 °C. The analysis was performed using acetonitrile and water (60:40 v/v containing 0.01% formic acid) as the mobile phase with a flow rate of 0.5 mL/min, and injection volume was 5 µL. The Waters ACQUITY™ XevoQToF Spectrometer (Waters Corp.) was connected to the UPLC system via an electrospray ionization (ESI) interface. This source was operated in positive ionization mode with the capillary voltage at 1.5 kV at 100 °C and the temperature of the desolvation was 300 °C. The cone and desolvation gas flows were 40 L h^{-1} and 800 L h^{-1}, respectively. The collision gas flow and collision energy applied were 0.2 mL/min and 12 V, respectively. All data collected in Centroid mode were acquired using Masslynx™ software (Waters Corp.). Leucine-enkephalin was used at a concentration of 500 pg/µL as the

lock mass generating an $[M+H]^+$ ion (m/z 556.2771) and fragment at m/z 120.0813 and flow rate of 50 µL/min to ensure accuracy during the MS analysis.

Steady-state absorption spectra were recorded in a JASCO V-760 spectrophotometer. Laser Flash Photolysis (LFP) measurements were performed using a pulsed Nd:YAG L52137 V LOTIS TII at the excitation wavelength of 266 nm. The single pulses were ca. 10 ns duration, and the energy was ~12 mJ/pulse. The laser flash photolysis system consisted of the pulsed laser, a 77250 Oriel monochromator and an oscilloscope DP04054 Tektronix. The output signal from the oscilloscope was transferred to a personal computer. Absorbances of all solutions were adjusted at ~0.20 at 266 nm in acetonitrile. All UV and LFP measurements were done using 10×10 mm^2 quartz cuvettes at room temperature in deaerated conditions (25 min N_2 bubbling), using 10 mL of fresh solution in order to avoid data acquisition from photodegraded products. Control experiments indicated that the degree of decomposition of all oxetanes after photolysis was lower than 5%.

Femtosecond transient absorption experiments were performed using a pump-probe system. The femtosecond pulses were generated with a mode-locked Ti-Sapphire laser of a compact Libra HE (4 W power at 4 kHz) regenerative amplifier delivering 100 fs pulses at 800 nm (1 mJ/pulse). The output of the laser was split into two parts to generate the pump and the probe beams. Thus, tunable femtosecond pump pulses were obtained by directing the 800 nm light into an optical parametric amplifier. In the present case, the pump was set at 280 nm and passed through a chopper prior to focus onto a rotating cell (1 mm optical path) containing the samples in organic solution. The white light used as probe was produced after part of the 800 nm light from the amplifier travelled through a computer controlled 8 ns variable optical delay line and impinge on a CaF_2 rotating crystal. This white light was in turn split in two identical portions to generate reference and probe beams that then were focused on the rotating cell containing the sample. The pump and the probe beams were made to coincide to interrogate the sample. The power of the pump beam was set to 180 µW. Under these conditions, the degree of photodegradation of all oxetanes was lower than 5%. A computer-controlled imaging spectrometer was placed after this path to measure the probe and the reference pulses to obtain the transient absorption decays/spectra. The experimental data were treated and compensated by the chirp using the ExciPro program.

Steady-state photolysis. Irradiations were performed in a Luzchem multilamp photoreactor emitting at λ_{max} = 350 nm (12 × 8 W lamps). Solutions containing the uracil or thymine derivative (0.1 M) and BP (0.2 M) were irradiated through Pyrex for *ca*. 6h; the crude products containing the HH- and HT-oxetanes were purified by silica gel chromatography (hexane:ethyl acetate 80:20 v/v).

Oxetane HH-1. ^{1}H NMR (400 MHz, $CDCl_3$) δ 7.44-7.29 (m, 10H), 5.20 (d, *J* = 8.8 Hz, 1H), 4.94 (d, *J* = 8.8 Hz, 1H), 3.04 (s, 3H), 3.01 (s, 3H); ^{13}C NMR (100 MHz, $CDCl_3$) δ 167.0, 151.7, 143.3, 138.7, 128.7, 128.4, 128.3, 128.2, 125.9, 125.1, 96.0, 70.6, 60.7, 35.4, 27.3; HRMS (ESI): *m/z* calcd. for $C_{19}H_{19}N_2O_3$ $[M+H]^+$: 323.1396, found: 323.1391

Oxetane HH-2. ^{1}H NMR (400 MHz, $CDCl_3$) δ 7.44-7.26 (m, 10H), 5.24 (d, *J* = 8.8 Hz, 1H), 5.02 (d, *J* = 8.8 Hz, 1H), 4.47 (d, *J* = 17.6 Hz, 1H), 3.77 (s, 3H), 3.37 (d, *J* = 17.6 Hz, 1H), 3.06 (s, 3H); ^{13}C NMR (100 MHz, $CDCl_3$) δ 168.9, 166.6, 151.9, 142.5, 138.4, 128.7, 128.5, 128.4, 126.1, 125.4, 95.3, 70.2, 59.4, 52.7, 48.0, 27.5; HRMS (ESI): *m/z* calcd. for $C_{21}H_{21}N_2O_5$ $[M+H]^+$: 381.1450; found: 381.1446.

Oxetane HH-3. ^{1}H NMR (400 MHz, CD_3CN) δ 7.41-7.23 (m, 10H), 4.94 (s, 1H), 3.21 (s, 3H), 2.70 (s, 3H), 0.98 (s, 9H); ^{13}C NMR (100 MHz, $CDCl_3$) δ 169.7, 152.0, 144.2, 139.0, 128.3, 127.8, 127.6, 125.2, 124.4, 91.1, 83.5, 61.5, 35.8, 29.7, 27.4, 24.6; HRMS (ESI): *m/z* calcd. for $C_{23}H_{27}N_2O_3$ $[M+H]^+$: 379.2022; found: 379.2027.

Oxetane HT-3. ^{1}H NMR (400 MHz, CD_3CN) δ 7.84-7.20 (m, 10H), 5.84 (s, 1H), 3.17 (s, 3H), 2.66 (s, 3H), 0.96 (s, 9H); ^{13}C NMR (100 MHz, $CDCl_3$) δ 169.1, 153.0, 144.5, 128.2, 127.7, 127.4, 127.2, 125.9, 89.5, 84.3, 66.0, 35.9, 34.2, 29.7, 27.5; HRMS (ESI): *m/z* calcd. for $C_{23}H_{27}N_2O_3$ $[M+H]^+$: 379.2022; found: 379.2026.

Oxetane HH-4. ^{1}H NMR (400 MHz, $CDCl_3$) δ 7.37-7.23 (m, 10H), 4.97 (s, 1H), 4.84 (d, *J* = 17.6 Hz, 1H), 3.82 (s, 3H), 3.73 (d, *J* = 17.6 Hz, 1H), 2.84 (s, 3H), 1.10 (s, 9H); ^{13}C NMR (100 MHz, $CDCl_3$) δ 169.8, 169.1, 152.1, 143.7, 139.1, 128.7, 128.4, 127.8, 125.4, 124.6, 90.6, 83.6, 59.7, 52.6, 48.3, 36.2, 27.5, 24.4; HRMS (ESI): *m/z* calcd. for $C_{25}H_{29}N_2O_5$ $[M+H]^+$: 437.2076; found: 437.2071.

Oxetane HT-4. ^{1}H NMR (400 MHz, $CDCl_3$) δ 7.79-7.19 (m, 10H), 5.81 (s, 1H), 4.80 (d, *J* = 17.6 Hz, 1H), 4.07 (d, *J* = 17.6 Hz, 1H), 3.80 (s, 3H), 2.79 (s, 3H), 1.04 (s, 9H); ^{13}C NMR (100 MHz, $CDCl_3$) δ 169.2, 168.9, 152.0, 142.6, 141.4, 128.1, 127.8, 127.5, 127.3, 127.1, 126.0, 89.8, 83.3, 66.0, 52.5, 47.1, 36.1, 27.8, 27.3; HRMS (ESI): *m/z* calcd. for $C_{25}H_{29}N_2O_5$ $[M+H]^+$: 437.2076; found: 437.2073.

Oxetane HH-5. ^{1}H NMR (400 MHz, $CDCl_3$) δ 7.38-7.25 (m, 10H), 4.78 (d, *J* = 17.6 Hz, 1H), 4.64 (s, 1H), 3.79 (s, 3H), 3.58 (d, *J* = 17.6 Hz, 1H), 2.85 (s, 3H), 1.76 (s, 3H); ^{13}C NMR (100 MHz, $CDCl_3$) δ 169.0, 168.8, 151.9, 143.8, 138.6, 128.7, 128.4, 128.1, 125.6, 125.1, 91.3, 65.3, 52.7, 48.3, 27.5, 23.7; HRMS (ESI): *m/z* calcd. for $C_{22}H_{23}N_2O_5$ $[M+H]^+$: 395.1607; found: 395.1607.

Oxetane HT-5. ^{1}H NMR (400 MHz, $CDCl_3$) δ 7.55-7.18 (m, 10H), 5.29 (s, 1H), 4.64 (d, *J* = 23.6 Hz, 1H), 4.04 (d, *J* = 23.6 Hz, 1H), 3.78 (s, 3H), 2.78 (s, 3H), 1.52 (s, 3H); ^{13}C NMR (100 MHz, $CDCl_3$) δ 169.1, 151.7, 141.8, 141.1, 128.3, 128.0, 127.7, 127.6, 125.3, 125.1, 90.5, 87.1, 52.5, 46.1, 27.8, 20.1; HRMS (ESI): *m/z* calcd. for $C_{22}H_{23}N_2O_5$ $[M+H]^+$: 395.1607, found: 395.1606.

Conflicts of interest

There are no conflicts to declare.

Acknowledgements

Financial support from the Spanish Government (RYC-2015-17737 and CTQ2017-89416-R) and from the Consellería d'Educació Cultura i Esport (PROMETEO/2017/075 and GRISOLIAP/2017/005) is gratefully acknowledged.

References

1 K. H. Kraemer, *Proc. Natl. Acad. Sci. USA*, 1997, **94**, 11-14.
2 J.-S. Taylor, *Acc. Chem. Res.*, 1994, **27**, 76-82.
3 F. Urbach, *J. Photochem. Photobiol. B*, 1997, **40**, 3-7.
4 H. Mukhtar and C. A. Elmets, *Photochem. Photobiol.*, 1996, **63**, 356-357.
5 B. M. Sutherland, *Photochem. Photobiol.*, 1996, **63**, 375-377.
6 S. Tommasi, M. F. Denissenko and G. P. Pfeifer, *Cancer Res.*, 1997, **57**, 4727-4730.
7 J. Cadet, A. Grand and T. Douki, *Top. Curr. Chem.*, 2015, **356**, 249-275.

8 J. Cadet, S. Mouret, J. L. Ravanat and T. Douki, *Photochem. Photobiol.*, 2012, **88**, 1048-1065.
9 B. Epe, M. Pflaum and S. Boiteux, *Mutat. Res.*, 1993, **299**, 135-145.
10 J. Li, Z. Liu, C. Tan, X. Guo, L. Wang, A. Sancar and D. Zhong, *Nature*, 2010, **466**, 887-890.
11 T. Todo, H. Ryo, K. Yamamoto, H. Toh, T. Inui, H. Ayaki, T. Nomura and M. Ikenaga, *Science*, 1996, **272**, 109-112.
12 T. Todo, H. Takemori, H. Ryo, M. Ihara, T. Matsunaga, O. Nikaido, K. Sato and T. Nomura, *Nature*, 1993, **361**, 371-374.
13 T. Todo, H. Tsuji, E. Otoshi, K. Hitomi, S.-T. Kim and M. Ikenaga, *Mutat. Res.*, 1997, **384**, 195-204.
14 K. Surana, B. Chaudhary, M. Diwaker and S. Sharma, *Med. Chem. Commun.*, 2018, **9**, 1803-1817.
15 F. Bosca and M. A. Miranda, *J. Photochem. Photobiol. B*, 1998, **43**, 1-26.
16 T. Delatour, T. Douki, C. D'Ham and J. Cadet, *J. Photochem. Photobiol. B*, 1998, **44**, 191-198.
17 J. E. Rogers and L. A. Kelly, *J. Am. Chem. Soc.*, 1999, **121**, 3854-3861.
18 A. Blasco-Brusola, M. Navarrete-Miguel, A. Giussani, D. Roca-Sanjuán, I. Vayá and M. A. Miranda, *Phys. Chem. Chem. Phys.*, 2020, **22**, 20037-20042.
19 M. C. Cuquerella, V. Lhiaubet-Vallet, F. Bosca and M. A. Miranda, *Chem. Sci.*, 2011, **2**, 1219-1232.
20 P. Miró, M. Gómez-Mendoza, G. Sastre, M. C. Cuquerella, M. A. Miranda and M. L. Marín, *Chem. Eur. J.*, 2019, **25**, 7004-7011.
21 V. Vendrell-Criado, V. Lhiaubet-Vallet, M. Yamaji, M. C. Cuquerella and M. A. Miranda, *Org. Biomol. Chem.*, 2016, **14**, 4110-4115.
22 S. Encinas, N. Belmadoui, M. J. Climent, S. Gil and M. A. Miranda, *Chem. Res. Toxicol.*, 2004, **17**, 857-862.
23 A. Joseph and D. E. Falvey, *J. Am. Chem. Soc.*, 2001, **123**, 3145-3146.
24 A. Joseph, G. Prakash and D. E. Falvey, *J. Am. Chem. Soc.*, 2000, **122**, 11219-11225.
25 G. Prakash and D. E. Falvey, *J. Am. Chem. Soc.*, 1995, **117**, 11375-11376.
26 N. Belmadoui, S. Encinas, M. J. Climent, S. Gil and M. A. Miranda, *Chem. Eur. J.*, 2006, **12**, 553-561.
27 S.-T. Kim, K. Malhotra, C. A. Smith, J.-S. Taylor and A. Sancar, *J. Biol. Chem.*, 1994, **269**, 8535-8540.
28 A. Joseph and D. E. Falvey, *Photochem. Photobiol. Sci.*, 2002, **1**, 632-635.
29 J. A. Bell and H. Linschitz, *J. Am. Chem. Soc.*, 1963, **85**, 528-532.
30 A. Blasco-Brusola, I. Vayá and M. A. Miranda, *J. Org. Chem.*, 2020, ***Accepted, DOI: 10.1021/acs.joc.0c02088***
31 N. Tamai, T. Asahi and H. Masuhara, *Chem. Phys. Lett.*, 1992, **198**, 413-418.
32 W. M. Kwok, X. Guan, L. M. Chu, W. Tang and D. L. Phillips, *J. Phys. Chem. B*, 2008, **112**, 11794-11797.